# Accepted Manuscript

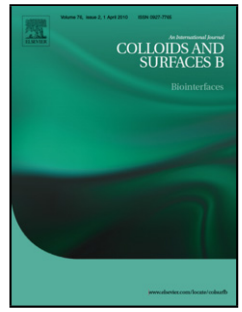


Title: Development of functionalized gold nanoparticles as nanoflare probes for rapid detection of classical swine fever virus

Authors: Pengbo Ning, Zhongxing Wu, Xuepeng Li, Yulu Zhou, Aoxue Hu, Xiaocheng Gong, Jun He, Yuqiong Xia, Kangkang Guo, Ruili Zhang, Xianghan Zhang, Zhongliang Wang

| | |
|---|---|
| PII: | S0927-7765(18)30471-5 |
| DOI: | https://doi.org/10.1016/j.colsurfb.2018.07.024 |
| Reference: | COLSUB 9480 |

To appear in: *Colloids and Surfaces B: Biointerfaces*

| | |
|---|---|
| Received date: | 28-1-2018 |
| Revised date: | 1-7-2018 |
| Accepted date: | 9-7-2018 |

Please cite this article as: Ning P, Wu Z, Li X, Zhou Y, Hu A, Gong X, He J, Xia Y, Guo K, Zhang R, Zhang X, Wang Z, Development of functionalized gold nanoparticles as nanoflare probes for rapid detection of classical swine fever virus, *Colloids and Surfaces B: Biointerfaces* (2018), https://doi.org/10.1016/j.colsurfb.2018.07.024

# Development of functionalized gold nanoparticles as nanoflare probes for rapid detection of classical swine fever virus

Pengbo Ning[1,2,*], Zhongxing Wu[1], Xuepeng Li[1], Yulu Zhou[4], Aoxue Hu[1], Xiaocheng Gong[1], Jun He[1], Yuqiong Xia[1,2], Kangkang Guo[3], Ruili Zhang[1,2], Xianghan Zhang[1,2] & Zhongliang Wang[1,2,*]

[1]School of Life Science and Technology, Xidian University, Xi'an, Shaanxi 710071, PR China

[2] Engineering Research Center of Molecular and Neuro Imaging Ministry of Education, Xi'an, Shaanxi 710071, PR China

[3] College of Veterinary Medicine, Northwest A&F University, Yangling, Shaanxi 712100, PR China

[4] College of life science, Wuhan University, Wuhan, Hubei 430072, PR China

* Correspondence to: Pengbo Ning, email: tommy0627@163.com; Zhongliang Wang, email: wangzl@xidian.edu.cn

Competing interests: The authors declare that they have no competing interests.

Graphical abstract

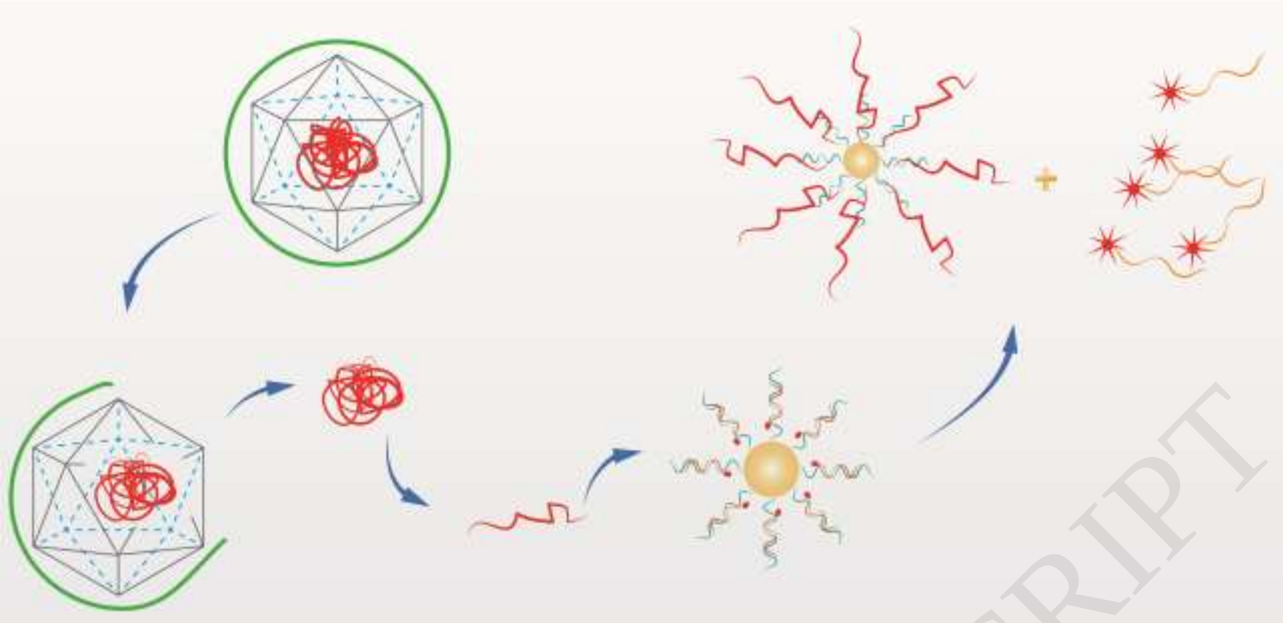

Highlights

- We synthesized gold nanoparticles as nanoflare probes for CSFV.
- No nucleic acid amplification was needed to achieve rapid CSFV detection.
- Quantitative analysis for virus nucleic acid was possible at concentrations as low as 50 pg/μL.
- Field sample detection offers possibilities for application in animal husbandry.

**Abstract:**

Classical swine fever (CSF) is a devastating viral disease affecting pigs that causes major economic losses worldwide. Conventional assays to identify classical swine fever virus (CSFV) face challenges, such as the required molecular amplification of the target molecules via polymerase chain reaction (PCR). We designed a gold nanoflare probe to directly detect CSFV. Gold nanoparticles (AuNPs) were conjugated with a pair of complementary DNA sequences that specifically recognized and captured CSFV RNA, resulting in a fluorescence signal to indicate the existence of CSFV. The constructed nanocomposite was then utilized in a quantitative analysis to recognize the virus sequence present at amounts as low as 50 pg/μL. The CSFV-AuNP probe enabled real-time, quantitative detection of native CSFV in response to doses of the specific RNA sequence (CSFV NS2) that indicated active viral replication of CSFV Shimen in macrophages after 12, 24, and 48 h. The potential diagnostic applications of the probe were demonstrated by measuring CSFV without nucleic acid amplification in samples from seven types of tissue samples, specifically heart, spleen, kidney, liver, lymph, intestine, and muscle samples obtained from one pig confirmed to suffer CSF. The speed, sensitivity, and versatility of this CSFV-AuNP biosensor make it an ideal candidate for further application in the prevention and control of animal epidemic

diseases.

**Keywords**: Gold nanoparticles, Classical swine fever virus, Detection, Nanoflares

## 1. Introduction

Classical swine fever (CSF) is a highly contagious disease affecting swine that is caused by classical swine fever virus (CSFV); it is classified as an OIE List A disease that has caused major damages to the swine industry [1]. Although some countries of the European Union have had some success in controlling the epidemic of CSF, infection by CSFV causes a major disease that endangers the pig-breeding industries of developing countries, including China [2]. Eradicating CSF is difficult because methods are still needed for both rapid and effective diagnosis and the monitoring of the occurrence and spread of CSF. CSF is characterized by hemorrhagic lymphadenitis, high fever, depression, and diffuse hemorrhaging of the skin, kidneys, and other organs. Although those symptoms are easily identified in a clinical diagnosis, CSFV is usually considered to be a potential infection in pigs before relying on clinical symptoms to rule out CSF [3]. Thus, the rapid detection of CSFV is of great significance for the diagnosis, early warning, and prevention of CSF.

Considering the hazards to the global pig-breeding industry caused by CSFV infection, researchers have performed exploratory research on detection technologies for CSFV, mainly based on three detection mechanisms. (1) Observation of virions. The presence of virus particles can be directly observed by electron microscopy, a technique that is regarded as the “gold standard” for virus detection [4]. The advantage of this technology is its direct detection of CSFV, but the equipment is expensive and observation is limited to research institutions. (2) Immunodiagnostic technique. As an antigen, CSFV can stimulate the host’s immune system to produce antibodies and also be neutralized by specific antibodies. Based on the characteristics of antigen–antibody binding, a number of methods for the detection of CSFV have been designed that utilize the enzyme-linked immunosorbent assay (ELISA) approach [5,6]. However, the high cost of antibody preparation and false-negative results are frequent problems preventing the use of this method to inspect a herd. (3) Detection of viral nucleic acid. As a pestivirus within the family *Flaviviridae*, CSFV has a single-stranded RNA genome of approximately 12,300 bases that can be detected soon after infection. Therefore, researchers have detected specific CSFV RNA sequences using different techniques in recent years, such as the polymerase chain reaction (PCR) [7] and quantitative polymerase chain reaction (qPCR) [8]. These methods quantitatively analyze viral nucleic acid by detecting specific nucleotides and greatly improve the sensitivity of these methods for the detection of CSFV. The problem with these approaches is the complication of extracting RNA from the diseased specimen; polluted or degraded RNA often yields false positive or false negative results.

Considering the continued risk of CSF to swine populations, an assay to identify and monitor this disease is urgently needed. Researchers have also realized that different methods have different limitations. Future detection methods for CSFV should be able to directly detect the virion with high sensitivity and wide availability. Gold nanoparticles (AuNPs) are widely used in biological imaging and other fields as target carriers [9], enhancers [10,11], and tracers [12,13] with special surface plasmon resonance properties, good biocompatibility, and high fluorescence quenching. Therefore, this work represents the latest international research progress in nanotechnology to establish a nanoflare model that achieves a breakthrough in the detection of CSFV. Specific RNA sequences of CSFV were demonstrated by fluorescence enhancement-based detection by the nanoflare. The detection of CSFV was successfully shown in CSFV-infected macrophages as well as different pathological tissue samples from a CSFV-positive pig, without using virus nucleic acid amplification. Our work facilitates the application of nanomaterials in virus detection for veterinary medicine.

## 2. Experimental section

### *2.1 Synthesis of nanoflares*

Two oligonucleotides, a recognition strand (5′-GUUGATGATATTGCGTACCUGAAAAAA-Thiol Modifier C3-S-3′) and a reporter strand (5′-Cy3-TCAGGTACGCAA-3′), were synthesized by Genscript Biotech Corporation (Suzhou, China). The two oligonucleotides were hybridized at a 1:1.2 molar ratio in phosphate-buffered saline (PBS). These oligonucleotides were heated at 75℃ for 0.5 h, and then the sample was cooled at room temperature while avoiding light to permit hybridization [14]. AuNPs were synthesized through the reduction of auric acid by sodium citrate, as described previously [15]. To synthesize nanoflares, a gold colloid solution (2.74 nM) was added to the preformed recognition-reporter DNA duplexes (822 nM) and then shaken for 12 h. PBS (10×; pH = 7.4) was added to the mixture to increase the concentration of NaCl gradually to 0.3 M over 8 h. The resulting nanoflares were centrifuged three times at 12 000 rpm for 15 min. The nanoflares were then suspended in PBS, protected from light, and stored at 4°C.

### *2.2 Characterization of nanoflares*

Transmission electron microscopy (TEM) measurements were performed on a JEOL 200X microscope operated at 200 kV to determine the particle size of the AuNPs. Dynamic light scattering (DLS) analysis was performed using a Zetasizer Nano ZS (Malvern Instruments Ltd., UK) to show the distribution of the hydrated particle size. The measurements of the ultraviolet–visible (UV/vis) spectra of AuNPs and nanoflares were performed using a TU-1900 spectrophotometer.

*2.3 Cell culturing and virus inoculation*

The CSFV Shimen strain was obtained from the Control Institute of Veterinary Bioproducts and Pharmaceuticals (Beijing, China). Porcine alveolar macrophages were maintained in RPMI 1640 medium (GE, USA) supplemented with 10% Fetal Bovine Serum (FBS) (Gibco Life Technologies, USA) at 37°C in 5% $CO_2$. The CSFV Shimen strain was added to the cultures at a multiplicity of infection (MOI) of 5 or 10 when the macrophages were 70%–80% confluent. Cellular RNA and protein were extracted 0, 12, 24, and 48 h after virus infection, as described in our previous work [16].

*2.4 PCR and qPCR*

The replication of CSFV was detected by the following specific oligonucleotide primers: 5'-GATCCTCATACTGCCCACTTAC-3' and 5'-GTATACCCCTTCACCAGCTTG-3' [8]. The PCR experiments used a total volume of 20 μL and were performed using a BioRad thermal cycler (Bio-Rad Laboratories, USA). The PCR thermal cycler program was 94°C for 5 min, 35 cycles at 94°C for 30 s, 60°C for 30 s, and a final extension at 72°C for 30 s. The 20-μL qPCR mixture contained 9 μL of SYBR® Premix Ex Taq™ II (Tiangen, China), 2 μL of cDNA, 2 μL of each primer, and 5 μL of RNase-free water. The reaction was performed in an Applied Biosystems 7300 Real-Time PCR System (Applied Biosystems, USA), and the qPCR thermal cycler program was 95°C for 2 min, 40 cycles at 95°C for 15 s, 55°C for 30 s, and a final extension at 68°C for 30 s.

*2.5 Western blotting*

Cells were washed three times with PBS and finally dispersed in RAPI Lysis Buffer (Beyotime, China) before performing a total protein extraction. The separation was performed at 100 V for 60 min in a 10% gel, with each well containing 20 μg of protein sample. After the separation, the proteins were transferred to polyvinylidenedifluoride (PVDF) membranes (Millipore, USA). After blocking for 1 h at room temperature (RT), the membranes were stained with mouse anti-E2 MAb (MssBio, China) at a 1:500 dilution and with β-actin (Biodragon Immunotech, China) at a 1:5000 dilution overnight at 4°C, followed by incubation with an HRP goat anti-mouse IgG (Jackson, America) at a 1:2000 dilution for 1 h at RT. Images were captured using the Gene Gnome XRQ Chemiluminescence Detector (Syngene, Cambridge, UK), and the densities of the protein bands were quantified by GeneSys software (VilberLourmat, France).

*2.6 Detection of CSFV using a fluorescence spectrophotometer*

Fluorescence signals were obtained using an F-7000 FL Spectrophotometer. A $\lambda_{ex}$ of 524 nm was used and the sample fluorescence was scanned in the range 540–800 nm with 5-nm steps. Samples were incubated for 5 min to allow the probe–target binding reaction to reach equilibrium. To confirm specificity, the nanoflare working reagent was prepared by adding 1 nM functionalized nanoflares in 100 μL PBS buffer to different concentrations of the CSFV target sequence (5′-CAGGTACGCAATATCATCAAC-3′). Each peak value reported was the average of three parallel experiments and expressed as mean ± standard deviation. Macrophages were infected with CSFV, and the amount of fluorescence at different time points was measured by adding 10 μL lysate of macrophages into 90 μL PBS buffer with 1 nM functionalized nanoflares. Each sample was measured in a separate cuvette to generate a peak fluorescence response to confirm the infection of CSFV. Tissue samples were frozen in liquid nitrogen and then subjected to tissue grinding. Measurements were performed when 10 μL of the ground tissue was added to a 90-μL nanoflare suspension (1 nM final nanoflare concentration). Each peak value was recorded using the same detection protocol as described above.

## 3. Results and Discussion

In this study, oligonucleotide-AuNP conjugates that possessed a highly specific sequence, designed and synthesized according to the target virus sequence, were developed to achieve real-time, quantitative detection of CSFV antigens. In our nanocomposite sensor for the detection of CSFV, AuNPs were conjugated with a pair of complementary DNA sequences, the recognition strand and reporter strand (Fig. 1A). The recognition strand was a thiolated CSFV-recognizing sequence, while the reporter strand was a thiolated sequence with a 5' end. In this CSFV-AuNP nanoflare probe, the fluorescence of the reporter strand was quenched due to fluorescence resonance energy transfer [18] between the fluorophore and the AuNP surface. Thus, the nanoflare was in a “turned-off” state in the absence of the targeted CSFV RNA. If CSFV was present, the recognizing strand would bind to the CSFV RNA and release the reporter strand, resulting in enhanced fluorescence intensity. When the nanoflare released the reporter strand, the sensor was in the “turned-on” state and could detect CSFV (Fig. 1B).

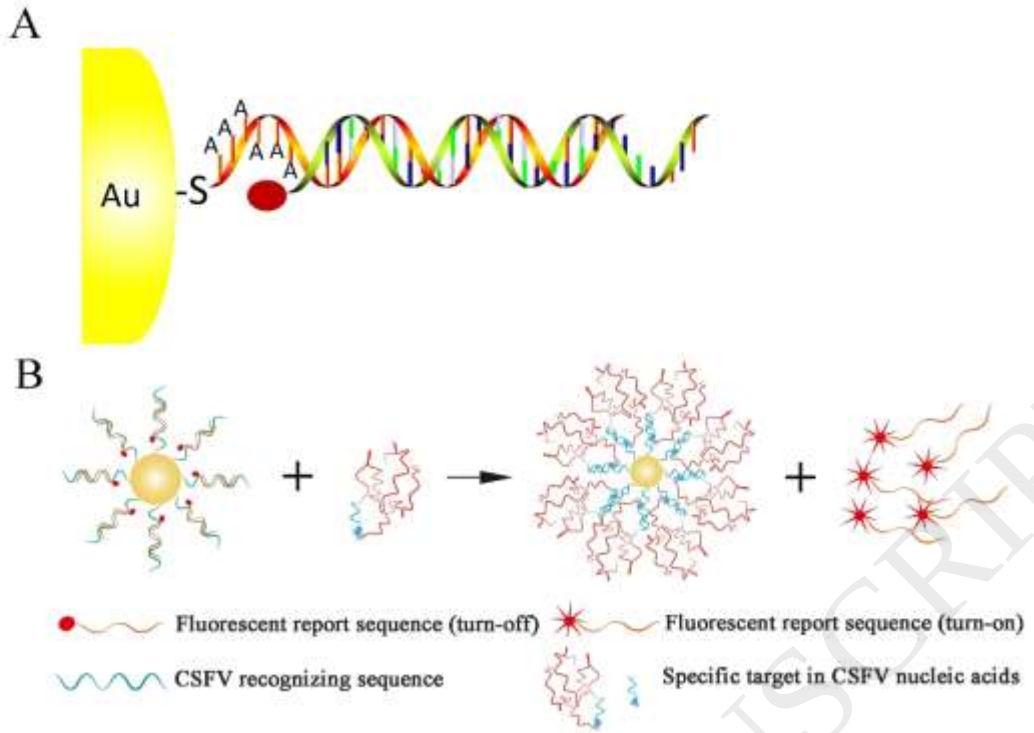


**Fig.1.** (A) Schematic illustration for the synthesis of nanoflares through AuNPs and thiolated recognition-reporter DNA duplexes. (B) Schematic representation of nanoflares by target detection.

The TEM image (Fig. 2A) shows that the prepared AuNPs were spherical and monodisperse. Their hydrodynamic diameter is approximately 30 nm as determined by DLS (Fig. 2B). The UV/vis spectra of the AuNPs and the nanoflare composite are similar and have a maximum absorption peak of 524 nm (Fig. 2C).

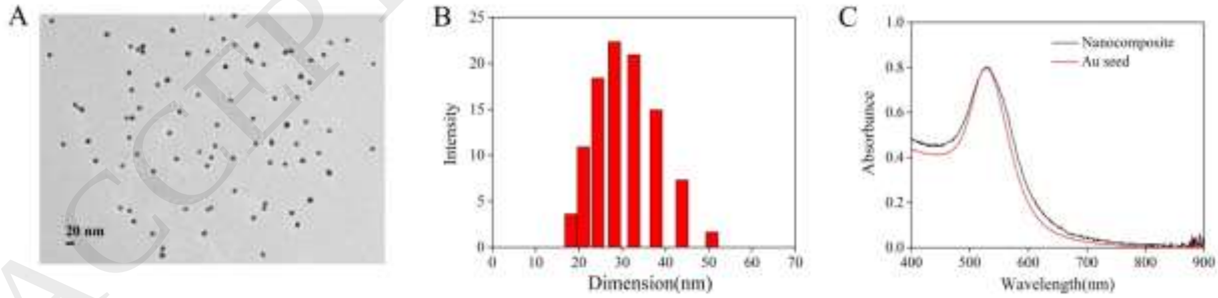


**Fig.2.** (A) TEM image of AuNPs. (B) The size distribution of AuNPs was measured by DLS. (C) UV-Vis absorbance of AuNPs and Nanoflares at 520 nm was detected.

The qualitative analysis shows that the fluorescence intensity is enhanced by approximately four times when the CSFV target sequence (1 μg) is added to the 1 nM CSFV-AuNP nanoflare solution (Fig. 3A). For the detection of CSFV, sensitivity is extremely important. The fluorescence intensity was measured with different concentrations of the CSFV target sequence in 1-nM CSFV-AuNP nanoflare solutions. These fluorescence measurements show the limit of detection of 0.05 pg/μL in the 1-nM CSFV-AuNPs nanoflare solution (Fig. 3B), indicating the high sensitivity of this technique when compared with time-consuming PCR [18] and qPCR [8] that require nucleic acid amplification of CSFV samples. The blast analysis showed that the sequence of the recognition strand was specific to bind CSFV in NCBI (https://blast.ncbi.nlm.nih.gov/Blast.cgi) (Fig. S1), and no significant fluorescence was produced in the presence of other viruses (PCV, PRV, and PRRSV) to which swine are particularly susceptible (Fig. S2), thus demonstrating the specificity of this CSFV-AuNP probe.

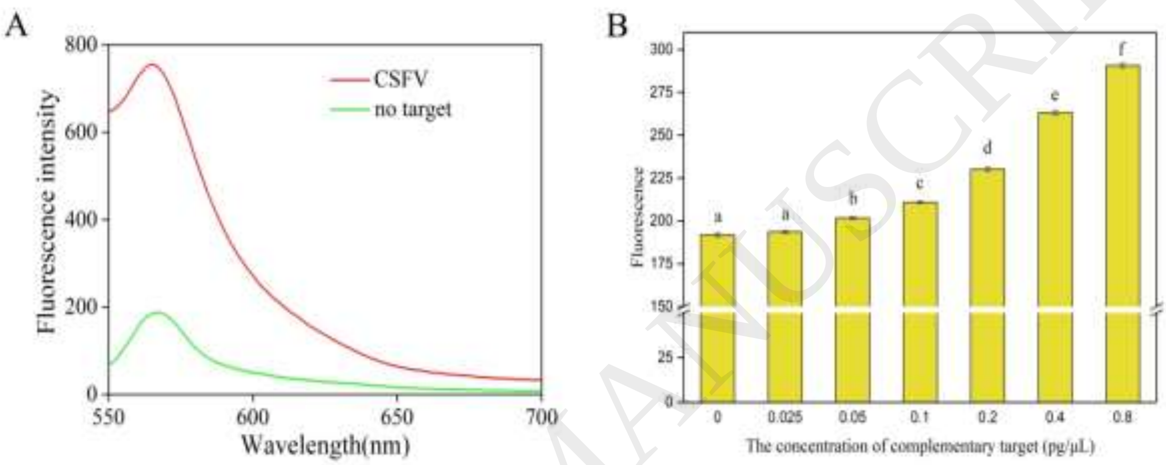


**Fig.3.** (A) Fluorescence spectra of nanoflares in the presence of no target (green line), CSFV target (red line). (B) Fluorescence intensity of the nanoflares (1nM) in the presence of various concentrations of complementary targets (0-0.8pg/μL). a ~ f indicates significant difference ($P<0.05$).

To observe the effect of the CSFV-AuNP probe in vitro, we infected macrophages with the CSFV Shimen strain at a MOI of 5 or 10 for 0, 12, 24, and 48 h. The conditioned media were collected, and then the CSFV-AuNP probe was added into the cell lysate to detect the change in fluorescence intensity. CSFV replication was measured at different time points by recording the fluorescence data. The results indicate that the signal increased significantly while the probe is in the cell lysate of the CSFV-infected macrophages compared to the results from mock-infected macrophages (Fig. 4A). A western blot analysis for the E2 protein of CSFV confirms the effective infection of the virus (Fig. 4B). Additionally, the results in Fig. 3A show that the concentrations of the CSFV Shimen strain in groups infected at an MOI of 10 are higher than those of groups infected at an MOI of 5 at each time point. Fluorescence measurements show that the replication of CSFV Shimen is significantly enhanced in a time- and dose- dependent manner, a result that is fully consistent with the qPCR results for the CSFV Shimen strain in macrophages (Fig. 4C).

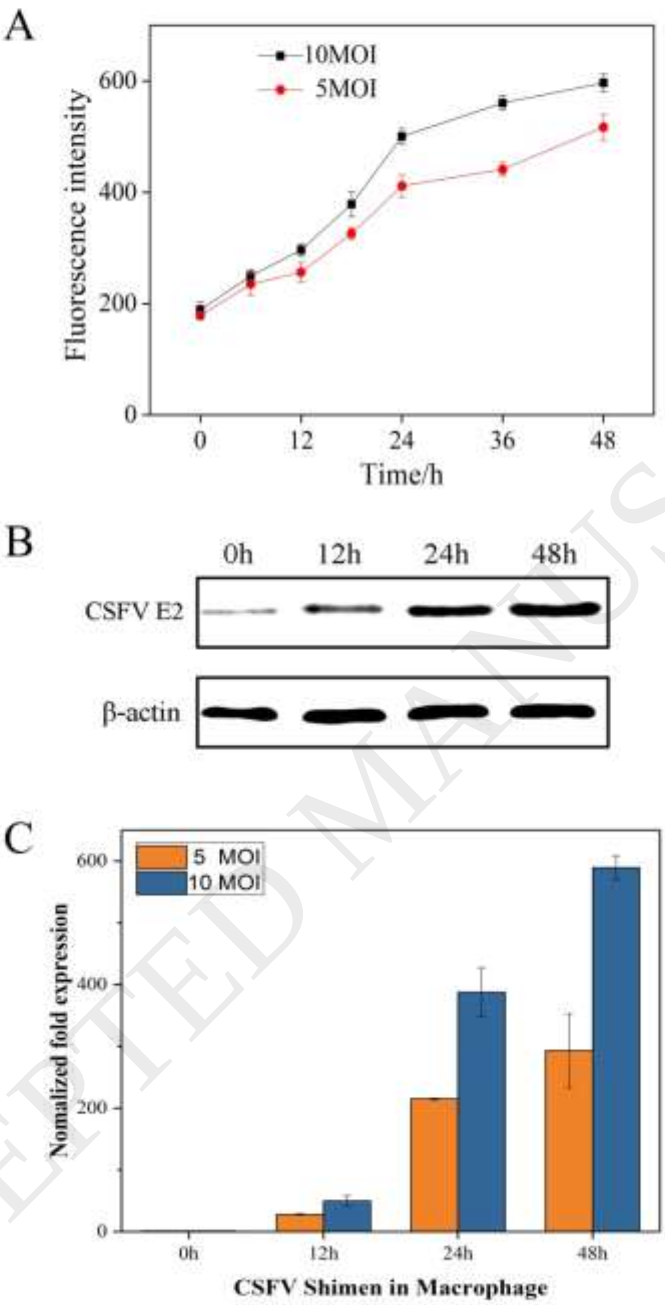


**Fig.4.** (A) Hybridization kinetics of nanoflares associated with CSFV Shimen strain at the 5 or 10 MOI for 0, 12, 24, 48h. (B) Western blot analysis of CSFV E2 protein expression levels for infected macrophages with CSFV Shimen strain at different time points. (C) qPCR analysis of E2 mRNA of CSFV expression levels for infected macrophages with 5 or 10 MOI CSFV Shimen strain at 0, 12, 24, 48h.

To provide a proof-of-concept for the CSFV-AuNP nanoflare technology, we tested the CSFV-AuNP probe on seven tissue samples, specifically heart, spleen, kidney, liver, lymph, intestine, and muscle samples obtained from one CSFV-infected pig with pathologically confirmed CSF. Infection by CSFV is additionally confirmed in each of the seven samples by PCR screening (Fig. 5A). In comparison, the fluorescence measurements also indicate CSFV infection after standardized tissue grinding of these seven samples, and no significant differences are found between the PBS samples and the control samples obtained from the CSFV-negative pig (Fig. 5B). More importantly, we notice a significant difference in the fluorescence data among the seven CSFV infected tissue samples, with the highest fluorescence in the lymph sample and the second-highest fluorescence in the spleen sample, in agreement with our previous study of different tissues infected by CSFV in vitro [19].

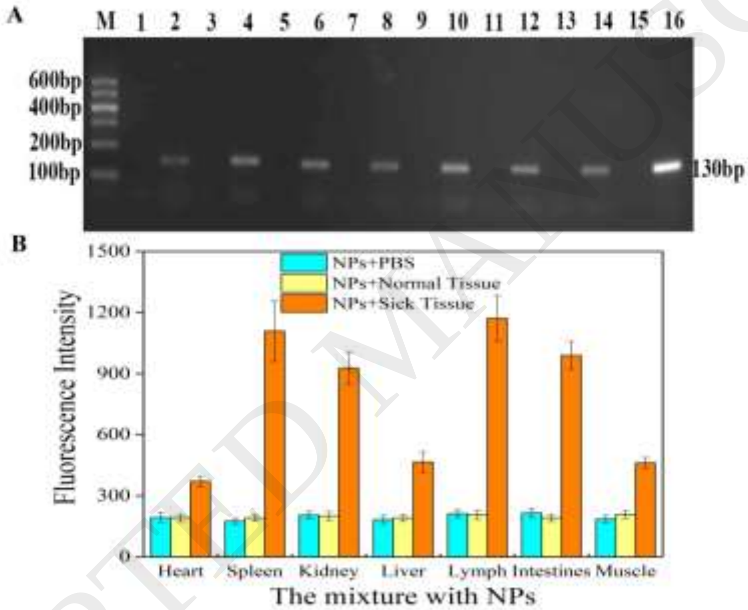


**Fig.5.** (A) Amplification product of the target fragment of CSFV. Note: DNA marker (M); the tissue from normal pig (line 1, heart; line 3, spleen; line 5, kidney; line 7, liver; line 9, lymph; line 11, intestines; and line 13, muscle, respectively); the tissue from CSFV infected pig (line 2, heart; line 4, spleen; line 6, kidney; line 8, liver; line 10, lymph; line 12, intestines; and line 14, muscle, respectively); negative control (line 15); and the CSFV amplification product (line 16). (B) Fluorescence intensities of major organs from normal pig and CSFV infected pig.

Researchers have elevated gene research by utilizing the unique advantages of AuNPs in recent years. Combining nanotechnology with RNA interference technology, a specifically designed nanozyme for hepatitis c virus (HCV) was bound to AuNPs to actively cleave HCV RNA in a sequence-specific manner and to perform a potent antiviral therapy [20]. Using Tubb3 and Fox3 mRNA from neural stem cells, Wang et al. (2014) [13] designed two complementary specific sequences of DNA to preferably bond to AuNPs as the carrier to demonstrate different expressions of Tubb3 and Fox3 in the differentiation of neural stem cells. In this study, when the CSFV-AuNP probe provided sequence-specific recognition, reporter oligonucleotides were released and fluorescence was measured quantitatively to demonstrate virus expression.

Virus detection technology is important as an early warning system because few effective drugs are available to treat certain viral infections at present [21]. A virus consists of only one kind of nucleic acid molecule (DNA or RNA). This structural feature is conducive to nanomaterials that can be developed to diagnose infectious diseases such as HCV [22], human papillomavirus [23], influenza virus [24], and Zika virus [25]. To the best of our knowledge, our CSFV-AuNP probe is the first to use nanoflares in combination with specific viral nucleic acid sequences for the rapid and accurate identification of CSFV in field samples. The key characteristics of this nanoflare technology are the elimination of time-consuming nucleic acid amplification and a turn-off/on effect in viral detection. Stable supplies of animal-derived products are closely related to both the development of the stockbreeding economy and the stability of the food system and human health [26]. Compared to human medicine, veterinary medicine is perceived as having lower entry requirements; it uses brief programs of administration for new diagnostic tests that offer more possibilities for the application of nanomaterials in viral detection.

## 4. Conclusions

The present study illustrates the application of oligonucleotide-AuNP nanotechnology in obtaining a CSFV-AuNP probe that provides rapid, specific, sensitive, and accurate determination of the CSFV nucleic acid in lab and field samples, without virus nucleic acid amplification. This work facilitates early warning, diagnosis, and prevention of CSF and provides a nanoflare technology as a reference for virus detection in animal husbandry.

## Acknowledgements

This work was supported by the National Natural Science Foundation of China (31470535), the National 1000 Young Talents Program of China and National Natural Science Foundation of Shaanxi Province under Grant (No. 2018JM2041). Thanks to Mr. Chengbo Wang for collecting samples.

## References

[1] V. Moennig, Introduction to classical swine fever: virus, disease and control policy, J. Vet. Microbio. 73 (2000) 93-102.

[2] D.J. Paton, I. Greiser-Wilke, Classical swine fever–an update, Res. Vet. Sci. 75 (2003) 169-178.

[3] A. Boklund, N. Toft, L. Alban, A Uttenthal, Comparing the epidemiological and economic effects of control strategies against classical swine fever in Denmark, Prev. Vet. Med. 90 (2009) 180-193.

[4] A. Calderaro, M.-C. Arcangeletti, I. Rodighiero, M. Buttrini, C. Gorrini, F. Motta, D. Germini, M.-C. Medici, C. Chezzi, F.D. Conto, Matrix-assisted laser desorption/ionization time-of-flight (MALDI-TOF) mass spectrometry applied to virus identification, Sci. Rep. (2014) 4.

[5] S.W. Seo, S.Y. Sunwoo, B.H. Hyun, Y.S. Lyoo, Detection of antibodies against classical swine fever virus in fecal samples from wild boar, Vet. Microbio. 161 (2012) 218-221.

[6] X. Li, L. Wang, X. Shi, D. Zhao, J. Yang, S. Yang, G. Zhang, Development of an immunochromatographic strip for rapid detection of antibodies against classical swine fever virus, J. Virol. Methods. 180 (2012) 32-37.

[7] Y. Jiang, H. Shang, H. Xu, L. Zhu, W. Chen, L. Zhao, L. Fang, Simultaneous detection of porcine circovirus type 2, classical swine fever virus, porcine parvovirus and porcine reproductive and respiratory syndrome virus in pigs by multiplex polymerase chain reaction, Vet. J. 183 (2010) 172-175.

[8] P. Ning, H. Li, W. Liang, K. Guo, X. Tan, W. Cao, L. Cheng, Y, Zhang, Detection and differentiation of classical swine fever virus strains C and Shimen by high-resolution melt analysis, J. Virol. Methods. 194 (2013) 129-131.

[9] F. Paciotti, L. Myer, D. Weinreich, D. Goia, N. Pavel, R.E. Mclauhlin, L. Takarmin, Colloidal gold: a novel nanoparticle vector for tumor directed drug delivery, Drug Delivery 11 (2004) 169-183.

[10] F. He, G. Yang, P. Yang, Y. Yu, R. Lv, C. Li , Y. Dai , S. Gai, J. Lin, A New Single 808 nm NIR Light - Induced Imaging - Guided Multifunctional Cancer Therapy Platform, Adv. Funct. Mat., (2015), 25(25):3966-3976.

[11] K. Selvaprakash, Y.C. Chen, Functionalized gold nanoparticles as affinity nanoprobes for multiple lectins, Colloids Surf. B Biointerfaces. 162 (2018) 60-68.

[12] D. Yang, G. Yang, P. Yang, R. Lv, S. Gai, C. Li, F. He, J. Lin, Assembly of Au Plasmonic Photothermal Agent and Iron Oxide Nanoparticles on Ultrathin Black Phosphorus for Targeted Photothermal and Photodynamic Cancer Therapy, Adv. Funct. Mat., (2017), 27(18):1700371.

[13] L. Feng, F. He, Y. Dai, B. Liu, G. Yang, S. Gai, N. Niu, R. Lv, C. Li, P. Yang, A Versatile Near Infrared Light Triggered Dual-Photosensitizer for Synchronous Bioimaging and Photodynamic Therapy, Acs Appl.Mater. Inter., (2017), 9(15):12993-13008.

[14] Z. Wang, R. Zhang, Z. Wang, H.-F. Wang, Y. Wang, J. Zhao, F. Wang, W. Li, G. Niu, D. O, et al, Bioinspired Nanocomplex for Spatiotemporal Imaging of Sequential mRNA Expression in Differentiating Neural Stem

Cells, ACS Nano 8 (2014) 12386-12396.

[15] K.C. Grabar, R.G. Freeman, M.B. Hommer, M.J. Natan, Preparation and Characterization of Au Colloid Monolayers, Anal. Chem. 67 (1995) 735–743.

[16] P. Ning, C. Hu, X. Li, Y. Zhou, A. Hu, Y. Zhang, L. Gao, C. Gong, K. Guo, X. Zhang, et al., Classical swine fever virus Shimen infection increases p53 signaling to promote cell cycle arrest in porcine alveolar macrophages, Oncotarget. 8 (2017): 55938.

[17] W. Pan, T. Zhang, H. Yang, W. Diao, N. Li, B. Tang, Multiplexed detection and imaging of intracellular mRNAs using a four-color nanoprobe, Anal. Chem. 85 (2013) 10581-10588.

[18] Y. Jiang, H. Shang, H. Xu, L. Zhu, W. Chen, L. Zhao, L. Fang, Simultaneous detection of porcine circovirus type 2, classical swine fever virus, porcine parvovirus and porcine reproductive and respiratory syndrome virus in pigs by multiplex polymerase chain reaction, Vet. J. 183 (2010) 172-175.

[19] P. Ning, L. An, W. Liang, Y. Zhang, Identification of inhibition of protein disulphide isomerase expression related to classical swine fever virus infection by using real-time PCR analysis, Biotechnol. Biotechnol. Eq. 29 (2015) 564-569.

[20] Z. Wang, H. Liu, S.H. Yang, T. Wang, C. Liu, Y.C. Cao, Nanoparticle-based artificial RNA silencing machinery for antiviral therapy, P. Natl. Acad. Sci. 109 (2012) 12387-12392.

[21] C.N. Hayes, K. Chayama, Why highly effective drugs are not enough: the need for an affordable solution to eliminating HCV, Expert Rev. Clin. Pha. 10 (2017) 583-594.

[22] L.L. Liu, X.Y. Wang, Q. Ma, Z.H. Lin, S.F. Chen, Y. Li, L.H. Lu, H.P. Qu, X.G. Su, Multiplex electrochemiluminescence DNA sensor for determination of hepatitis B virus and hepatitis C virus based on multicolor quantum dots and Au nanoparticles, Anal. Chim. Acta. 916 (2016) 92–101.

[23] A.M.J. Jimenez, M.A.M. Rodrigo, V. Milosavljevic, S. Krizkova, P. Kopel, Z Heger, V. Adam, Gold nanoparticles-modified nanomaghemite and quantum dots-based hybridization assay for detection of HPV, Sens. Actuators B: Chem. 240 (2017) 503-510.

[24] O. Adegoke, T. Kato, E.Y. Park, An ultrasensitive alloyed near-infrared quinternary quantum dot-molecular beacon nanodiagnostic bioprobe for influenza virus RNA, Biosens. Bioelectro. 80 (2016) 483–490.

[25] S. Afsahi, M.B. Lerner, J.M. Goldstein, J Lee, X. Tang, D.A. Bagarozzi Jr, D. Pan, L. Locascio, A. Walker, F. Barron, et al, Novel graphene-based biosensor for early detection of Zika virus infection, Biosens. Bioelectro. 100 (2018) 85-88.

[26] M.E. Dasenaki, N.S. Thomaidis, Meat Safety: II Residues and Contaminants, In Lawrie's Meat Science (Eighth Edition). (2017) 553-583.